Research Paper

Journal of Engineering and Technological Sciences

Reading Method and Experimental Evaluation of the UWB System D-DWM-PG3.6 for Local Positioning

Thuan-Tien Tran[1], Quoc-Thanh Tra[2], Chi-Ngon Nguyen[1], Phuong-Lan Tran-Nguyen[2], & Quoc-Khanh Huynh[2,*]

[1]Nam Can Tho University, 168 Nguyen Van Cu Street, An Binh Ward, Can Tho City, 94118, Vietnam
[2]Can Tho University, Campus II, 3/2 Street, Ninh Kieu Ward, Can Tho City, 94115, Vietnam

*Corresponding author: hqkhanh@ctu.edu.vn

Abstract

The UWB D-DWM-PG3.6 is a standalone positioning system based on Decawave's (now Qorvo) ultra-wideband technology. It is designed for local positioning without requiring satellite data systems, making it effective in areas with weak or unstable GPS signals. This study focuses on developing a method for reading and filtering data from the UWB system to obtain stable position parameters. Outlier data are removed, and filtering by moving average helps to smooth and stabilize the position data. Experiments were conducted in a 40×30 m space to evaluate the method's accuracy. The results show an average positioning error of 7.1 ± 3.6 cm, with a maximum of 26.9 cm under obstructed conditions. These findings highlight the potential for navigation applications in autonomous devices operating in enclosed spaces, such as warehouses and agricultural greenhouses, at a reasonable cost. However, the error magnitude indicates that the system should be integrated with ultrasonic sensors, recognition cameras, or laser technology to improve accuracy.

Keywords: *D-DWM-PG3.6; filtering; local positioning; reading; ultra-wideband.*

Introduction

Automation guided vehicles (AGV) contribute to cost reduction, lower the risk of workplace accidents, and enhance warehouse safety, particularly in large-scale, continuously operating facilities (Kubasakova et al., 2024; Koreis et al., 2025). However, a significant challenge for AGVs is accurate indoor positioning, as GPS is rendered ineffective by signal interference (Sakpere et al., 2017). Traditional positioning methods, such as optical, magnetic, or RFID sensors, offer high accuracy but require costly installations and fixed infrastructure, limiting system flexibility in warehouses with evolving layouts (Mo & Lee, 2011; Li et al., 2024; Rajab & Wang, 2024; Saengudomlert et al., 2025).

In recent years, the demand for indoor positioning systems (IPS) has increased significantly due to the development of applications in many fields such as autonomous robots, asset tracking, indoor navigation, security surveillance, and healthcare (Sanchez et al., 2012; H. Wang et al., 2024; Saeidi et al., 2025). Versus outdoor GPS-based positioning systems, indoor positioning systems face more challenges due to the presence of obstacles, multipath, and signal interference. Among the current indoor positioning technologies, ultra-wideband (UWB) positioning stands out for its centimeter-level accuracy and strong performance in environments with many obstacles (Z. Wang et al., 2018; K. Hassan et al., 2022; Ruiz et al., 2024; Tran et al., 2024; Xu et al., 2025).

The D-DWM-PG3.6 system, developed by Decawave (now Qorvo), is one of the most popular UWB solutions for distance measurement and local positioning (Decawave, 2021). It operates by measuring the time of flight (ToF) or time difference of arrival (TDoA) of radio signals between transmitters and receivers, from which to calculate distances (H. Chen et al., 2025; Lyu et al., 2025). With time measured to the picosecond, this system can achieve accuracy below 10 cm under ideal conditions, making it suitable for many applications (Boquet et al., 2024).

Moreover, as demand continues to grow for more flexible and cost-effective indoor navigation solutions, UWB technology is gaining attention for its scalability and robustness in dynamic environments (Sullivan et al., 2022; Zhang et al., 2022; Esmaeili-Yadaki & Khani, 2024; Cho et al., 2025). Unlike systems that rely on fixed infrastructure, UWB can

ISSN: 2337-5779
J. Eng. Technol. Sci. Vol. 58, No. 2, 2026, 514-523
DOI: 10.5614/j.eng.technol.sci.2026.58.4.4

DOI: 10.5614/j.eng.technol.sci.2026.58.4.4

adapt to changing layouts and varying environmental conditions, providing a competitive edge in logistics and manufacturing (Huang et al., 2017; Janousek et al., 2024; Ma et al., 2024). This adaptability makes UWB promising for next-generation AGV systems where precision, reliability, and real-time responsiveness are critical.

The UWB D-DWM-PG3.6 system provides a data string indicating the location of the receiving station (Decawave, 2021). However, due to environmental instability, device accuracy limitations, and the positioning method, the returned values may contain errors. To address this, this study focuses on developing a data reading method, incorporating noise filtering and the removal of anomalous error values. Experimental evaluations are conducted to determine the actual error magnitude, serving as a foundation for designing guidance systems for indoor AGV vehicles.

Materials and Methods

The D-DWM-PG3.6 Positioning System

The D-DWM-PG3.6 system, provided by Decawave (Qorvo), consists of a base station, fixed stations, and mobile tags that are mounted on moving equipment for positioning. The fixed stations are installed at predefined coordinate locations, with a minimum of three stations required for positioning. To expand the positioning range and working area, the number of fixed stations can be increased up to 14, and the number of tags can be increased to 100.

The D-DWM-PG3.6 hardware is depicted in Figure 1. The same hardware is used for all of the base station, fixed stations, and tags, differing only in their configuration settings within the software.

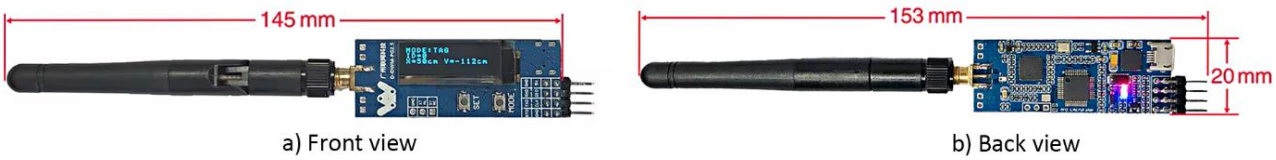

Figure 1 The D-DWM-PG3.6 devices (Decawave, 2021).

The distance d between two devices is calculated from the ToF principle and follows the equation in Eq. (1), (Han et al., 2021; Qorvo, 2025):

$$d = \frac{c \times (t_{round} - t_{reply})}{2} \tag{1}$$

where: c is the signal transmission speed in the air, tround is the total time from send to receive the signal, and treply is the processing time at the stations.

The distances are then used to triangulate the tag position relative to the base station.

Reading and Filtering the Output Location Data from UWB

After the system is set up, data from the tag is read through the USB port or Rx–Tx. It is in the form of a string as follows:

“b'Rtls: X=326cm,Y=204cm,Z=123cm \r\n”

If the system is set up in 2D mode, the return string is simpler:

“b'Rtls: X=326cm,Y=204cm \r\n”

The values right after X= and Y= are extracted and assigned, respectively, to the X and Y coordinates of the tag.

The reading process for one tag is described in Figure 2. When the process starts, the system will read data n times to calculate the tag’s mean initial position (X, Y), see Eq. (2).

$$X = \frac{\sum_{i=1}^{n} X_i}{n} \quad and \quad Y = \frac{\sum_{i=1}^{n} Y_i}{n} \tag{2}$$

where n is the filter window size. When a new position (X_{i+1}, Y_{i+1}) is recorded, the displacement ddis of this new coordinate from the previous position (X_i, Y_i) is calculated as follows in Eq. (3):

$$d_{dis} = \sqrt{(X_{i+1} - X_i)^2 + (Y_{i+1} - Y_i)^2} \tag{3}$$

Assume that these tags are attached to a mobile device, that moves a given maximum speed V_{lim}. The sampling period t_{sam} is the time between two consecutive data readings. Thus, the maximum movement d_{lim} in the sample time t_{sam} is described in Eq. (4):

$$d_{lim} = V_{lim} \times t_{sam} \tag{4}$$

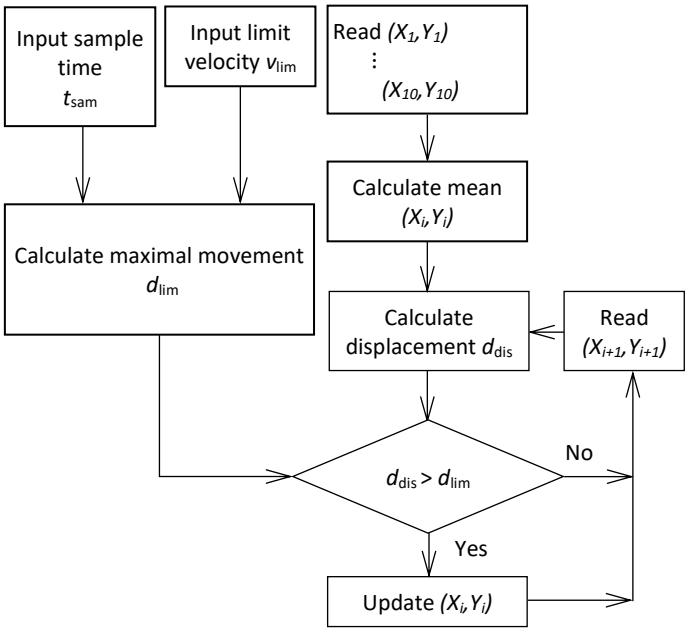

Figure 2 The reading and filtering process.

Under the speed-cap assumption, in Eq. (5), the tag cannot move further than d_{lim} during time t_{sam}. Thus, if

$$d_{lim} < d_{dis} \tag{5}$$

then the new value (X_{i+1}, Y_{i+1}) is considered as an error and is discarded. Otherwise, it will be updated using the moving average filtering method (Smith, 1999; Y. Chen et al., 2017). The oldest data point in Eq. (2) will be removed, and the new one (X_{i+1}, Y_{i+1}) will be added as the newest in the set of n most recent points to calculate the new position as in Eq. (6):

$$X_{update} = \frac{\sum_{i=1}^{n} X_{i+1}}{n} \quad and \quad Y_{update} = \frac{\sum_{i=1}^{n} Y_{i+1}}{n} \tag{6}$$

Experiment Setup

To evaluate the positioning accuracy achieved with the proposed data reading and filtering method, a D-DWM-PG3.6 system was deployed in an open field measuring 40 m×30 m. An orthogonal layout was selected due to the simple geometry, notably for accurate right-angle verification using the Pythagorean theorem. For the rectangular 40 m×30 m test area, the diagonal distance between the two endpoints must be exactly 50 meters. As shown in Figure 3, the positioning system consists of a base station and three fixed stations positioned at the corners of the test field. A mobile station (carrying a tag), connected to a laptop computer, is used to collect data and move between test points.

The spacing between the base stations was determined based on both the manufacturer's recommended optimal operating range for the D-DWM-PG3.6 UWB device and the practical limitations of the experimental setup: the test area restricts the distance between a tag and a base station to 40 m, equivalent to approximately 80% of the system's most stable range. This configuration enables a reliable evaluation of the system's performance under near-optimal conditions.

DOI: 10.5614/j.eng.technol.sci.2026.58.4.4

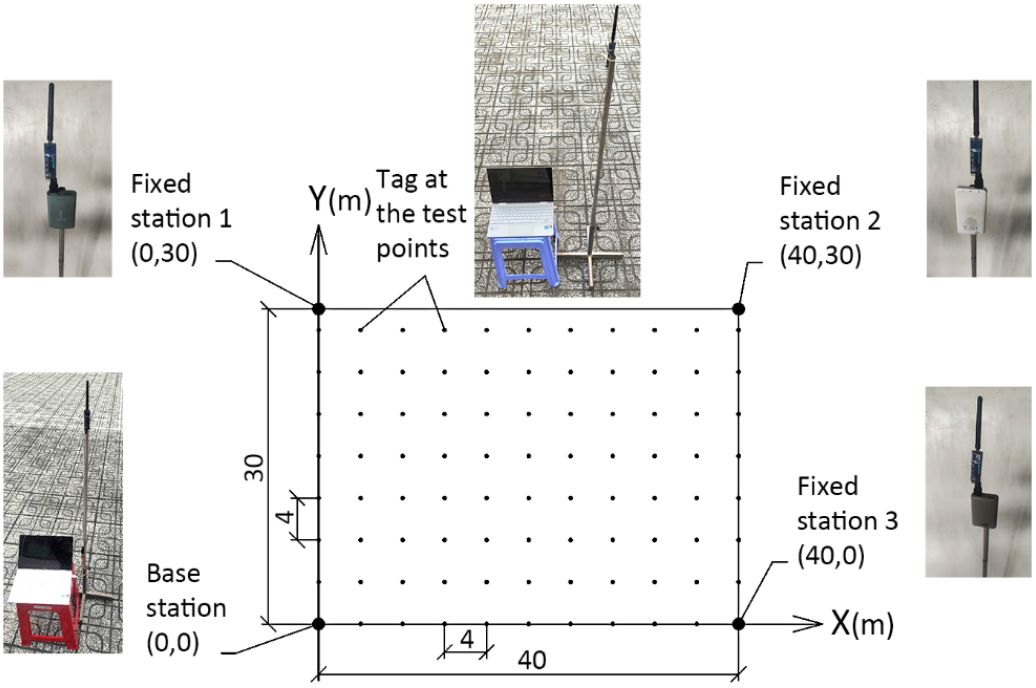

Figure 3 The experiment set up.

In strict accordance with installation guidelines, all base stations, fixed stations, and tags were mounted on vertical pillars with antennas oriented upward at a uniform height of 180 cm, as shown for the base station in Figure 3.

The test points are arranged in a grid pattern on the field, spaced at 4 m; there are 11 points horizontally and 8 points vertically. After removing the 2 points that coincide with the the base station and a fixed station, the total number of remaining checkpoints is 82.

The testing process entails the following steps:

Step 1: System initialization. Once the system is set up, the computer starts collecting data from the tag.
Step 2: Tag movement. The tag moves sequentially to each marked checkpoint on the floor.
Step 3: Data recording. At each test point, the coordinates are recorded 10 times before moving to the next one.
Step 4: Repetition for accuracy. After measurements have been taken at all test points, the tag returns to the starting point for the next round of measurements. Five rounds were conducted to ensure data reliability and consistency.

Thus, 50 position measurements are recorded at each of the 82 test points. The positions are then analyzed to assess the accuracy and performance of the positioning system.

Results

The position error ep in the 82 position measurements was calculated as the Euclidean distance between the mean measured tag locations ($X_{measure}$, $Y_{measure}$) and the corresponding test point positions (X_{tpoint}, Y_{tpoint}) , located by tape measurements:

$$e_p = \sqrt{\left(X_{measure} - X_{tpoint}\right)^2 + \left(Y_{measure} - Y_{tpoint}\right)^2} \tag{7}$$

The positioning errors ep for all 82 test points are presented in Table 1. The measurements yielded an average positioning error of 7.1±3.6 cm, with the maximum error reaching 13.8 cm. Figure 4 illustrates the distribution of the positioning errors along relative to the reference points, showing a slight tendency toward the positive axes, with a shift of approximately 1.7 cm in the X-direction.

Table 1 Positioning error (e_p) (cm).

Y (m)	*X* (m)									
	4	**8**	**12**	**16**	**20**	**24**	**28**	**32**	**36**	**40**
4	10.0	12.0	7.7	6.8	3.9	2.2	0.5	7.4	7.9	5.7
8	0.4	1.8	6.2	10.0	10.1	1.2	13.8	12.1	8.0	8.3
12	5.1	6.2	3.6	1.7	1.9	1.9	5.6	2.9	10.2	8.3
16	7.3	1.8	3.2	3.5	11.5	10.3	10.6	7.5	9.6	5.4
20	5.2	7.8	10.3	8.3	6.2	5.6	9.2	10.0	10.7	7.0
24	5.8	7.5	7.9	13.8	11.8	11.1	6.6	6.9	7.2	5.7
28	9.1	13.6	4.6	8.3	6.9	1.8	3.6	2.2	12.1	8.6
Mean	7.1 ± 3.6 (cm)									

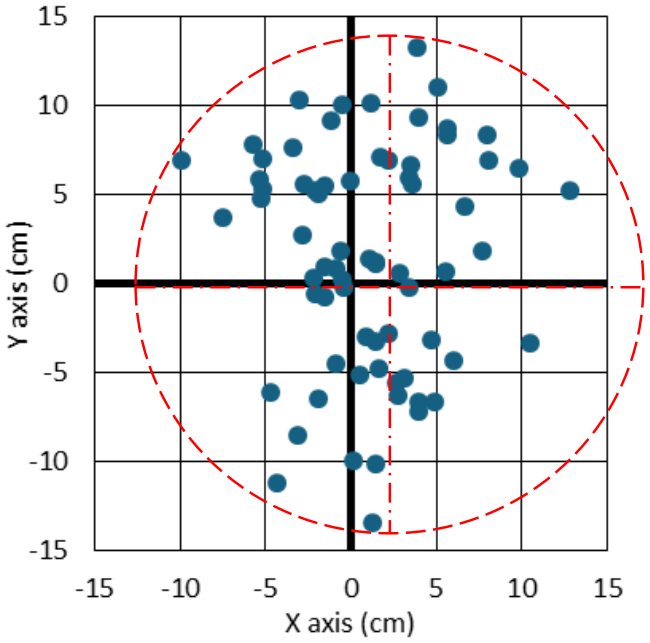

Figure 4 The positioning error (e_p) distribution.

At Y = 24 m, the mean positioning error in the X-direction was the largest at 8.4 cm, and this line was, therefore, selected to analyze the variation of errors with distance along the X axis. As shown in Figure 5, the positioning error along a single direction fluctuates around 5 cm, which is consistent with manufacturer specifications for one-dimensional estimates. In comparison, the two-dimensional error is larger, as reflected in Table 1. The positioning error values, whether positive or negative, appear to be almost random. Additionally, the standard deviation is approximately equal to the average error, at ± 2.3 cm.

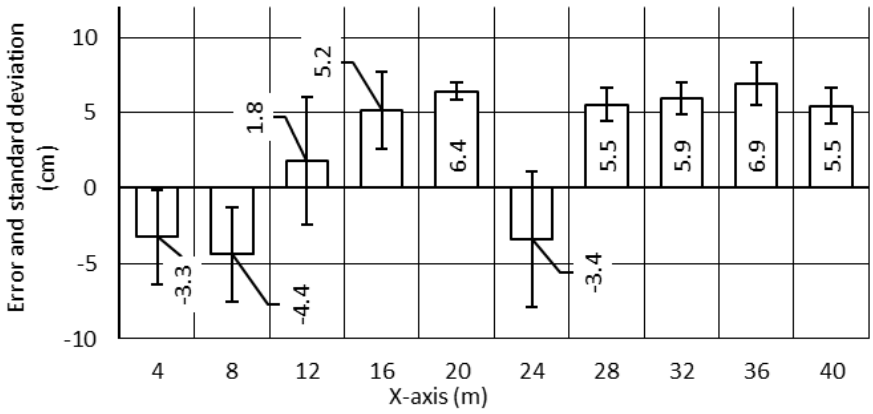

Figure 5 Positioning errors (e_p) vs. distance in *X*-direction.

DOI: 10.5614/j.eng.technol.sci.2026.58.4.4

The system was further evaluated in an obstacle-rich environment at six selected test points (Figure 6); the corresponding errors are summarized in Table 2. The mean positioning error increased to 14.8 ± 6.9 cm, and the error peaked at 26.9 cm when lines of sight to three of the four fixed stations were obstructed.

Figure 6 Test environment with obstacles.

Finally, the effect of filter window size on trajectory smoothing was examined by moving the tag along a diagonal path followed by a zig-zag segment (Figure 7). Window sizes of 3, 7, and 11 data points were tested, with a sampling frequency of 10 Hz and a maximum velocity limit of vlim = 400 cm/s. The trajectory with a window size of 3 measurements exhibited noticeable fluctuations, while windows of 7 and 11 measurements significantly reduced jitter. Given the slow manual movement in this experiment, a window size of 11 was selected to ensure stable filtering performance.

Table 2 Positioning error (e_p) in obstacle environment.

	Positioning error in obstacle environment (cm)					
X (cm)	600	300	600	300	300	−300
Y (cm)	300	1,050	150	1,200	600	450
e_p (cm)	8.8	15.6	10.1	9.6	26.9	17.6
$\bar{e}_p$ (cm)	14.8 ± 6.9					

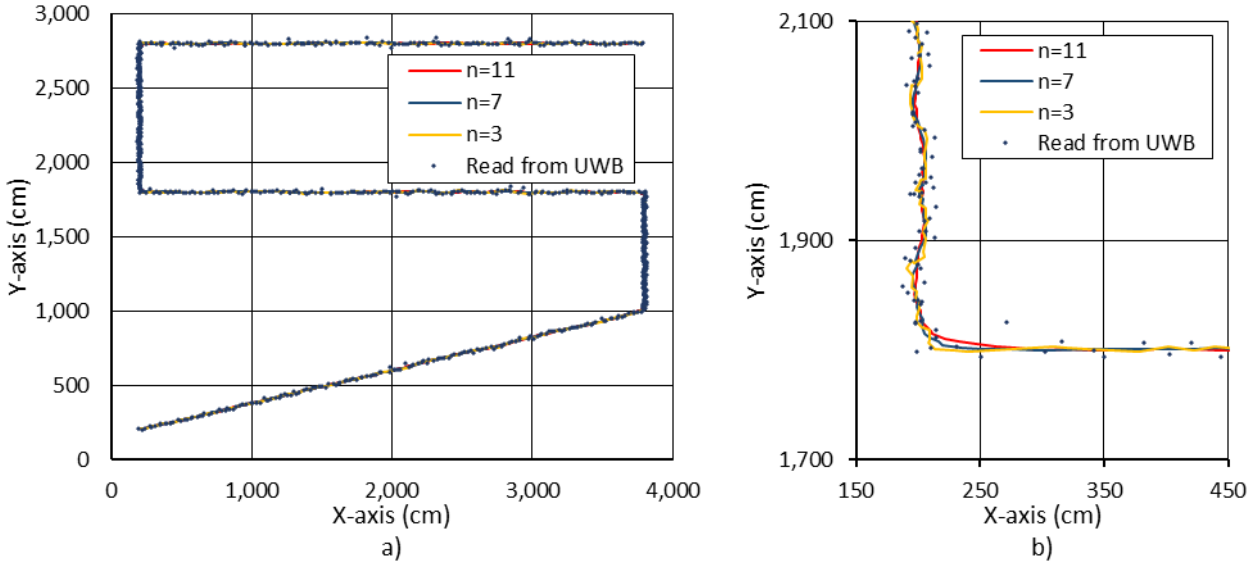

Figure 7 Effect of filter window size on the zig-zag trajectory at a sampling frequency of 10 Hz and V_{lim}= 400 cm/s.

Discussion

The experimental results indicate that the proposed reading and filtering method effectively stabilizes the coordinate measurements provided by the D-DWM-PG3.6 system. Although the average two-dimensional error of 7.1 cm is slightly higher than the manufacturer's nominal 5 cm accuracy (Decawave, 2021; Qorvo, 2025), such deviations are expected due to environmental factors, multipath propagation, and practical constraints in anchor placement. The slight directional bias observed in Figure 4 – approximately 1.7 cm toward the positive X-axis – suggests the presence of minor systematic effects, but the offset is small and does not indicate a strong tendency toward consistent overestimation or underestimation.

Comparative analysis reveals that moving average (MA) filtration achieved a competitive mean error of 7.1 cm, closely aligning with the previous 6.4 cm result (Ranjan et al., 2024). Crucially, our study extends validation by confirming the D-DWM-PG3.6 system's performance over a significantly larger and more comprehensive 40×30 m experimental field, utilizing 82 static points for a superior and highly realistic accuracy assessment.

The increase in positioning error under obstructed conditions (Table 2) confirms the susceptibility of UWB systems to non-line-of-sight (NLOS) conditions. Blocking the sight lines to fixed stations leaves the system with fewer measurements to rely on, degrading accuracy and causing significantly larger errors. Raising the height of the stations or adding additional fixed anchors may help to mitigate these effects in practical deployments.

The jitter in the raw trajectory originates primarily from high-frequency noise in the UWB measurements, caused by multipath propagation, small fluctuations in time-of-arrival estimation, and quantization effects. With a small window size (e.g., 3 points), the filter only weakly attenuates this noise, leading to noticeable oscillations in the estimated path, as shown in Figure 7. Increasing the window to 7 or 11 points enhances the low-pass effect, effectively suppressing high-frequency components for greater smoothing. Excessively large windows introduce a moderate response delay, reflecting the trade-off between noise reduction and motion responsiveness. These well-known filtering characteristics are especially important in practical deployments, where excessive jitter can cause AGVs or greenhouse robots to misinterpret their position, produce unstable steering commands, or deviate from planned paths, ultimately reducing operational accuracy and safety.

Limitations and future work

Comparing Tables 1 and 2 indicates that positioning accuracy decreased in cluttered environments, with an average error of 14.8 ± 6.9 cm—twice that observed in open spaces—suggesting value in mitigating the influence of obstacles through integration with supporting sensors, such as ultrasonic, laser, or vision-based devices.

Despite the promising results, several limitations should be acknowledged. First, the evaluation focused on two-dimensional positioning because accurate reference measurements for vertical coordinates were not feasible within the experimental environment. Second, only moving-average filtering was implemented; more advanced approaches, such as adaptive Kalman filtering or multimodal sensor fusion, could further reduce noise, particularly in dynamic or NLOS-prone settings. Finally, the trajectory experiments were conducted at relatively slow manual speeds, leaving high-speed performance untested.

Future research will address these limitations by extending the method to three-dimensional positioning, integrating UWB radio positioning with complementary sensors such as IMU and vision-based tracking, and implementing adaptive or model-based filtering methods to improve robustness under rapid motion and severe NLOS conditions. Additional studies will also consider expanding the number of fixed anchors, optimizing spatial layouts, and evaluating system performance in real AGV and greenhouse automation scenarios to support reliable and cost-effective indoor localization platforms.

Conclusion

This study proposed and experimentally validated a data reading and filtering method for the D-DWM-PG3.6 UWB positioning system, demonstrating that the combination of outlier removal and moving-average smoothing effectively stabilizes raw measurements and improves the consistency of reported coordinates. Experiments conducted over 82 grid points in a 40 × 30 m field yielded an average positioning error of (7.1 ± 3.6) cm under open conditions, while tests with obstacles resulted in a higher average error of (14.8 ± 6.9) cm, revealing the system's sensitivity to NLOS interference and anchor-geometry degradation. These findings confirm that the D-DWM-PG3.6 platform is suitable for

DOI: 10.5614/j.eng.technol.sci.2026.58.4.4

indoor localization tasks in logistics, warehousing, and greenhouse automation, particularly when complemented with additional sensing technologies to mitigate uncertainties in complex environments.

Future research will extend the method to full three-dimensional positioning, explore sensor-fusion schemes integrating IMU and vision-based systems, and develop adaptive filtering strategies to enhance robustness under high-speed motion and severe NLOS conditions, ultimately supporting the deployment of reliable and cost-effective localization solutions for next-generation autonomous platforms.

Nomenclature

c	signal transmission speed in the air
d	distance between two stations
d_{lim}	maximum limit movement
e_p	positioning error
n	filter window size
t_{round}	signal round trip duration
t_{reply}	processing time at the stations
t_{sam}	sampling period
v_{lim}	maximum speed of vehicle
(X, Y)	station or tag position
(X_i, Y_i)	previous position
(X_{i+1}, Y_{i+1})	new position
($X_{measure}$, $Y_{measure}$)	measured position
(X_{tpoint}, Y_{tpoint})	test points position
(X_{update}, Y_{update})	updated position

Acknowledgements

Thanks to Professor Wei-Chih Lin from National Sun Yat-sen University, Taiwan, for his support in providing the UWB system for the experiments.

Declaration of Generative AI and AI-Assisted Technologies in the Writing Process

During the preparation of this work, the author used chatGPT and chatDeepseek in order to correct grammar and language. After using this tool, the authors reviewed and edited the content as needed and take full responsibility for the content of the publication.

Compliance with ethics guidelines

The authors declare they have no conflict of interest or financial conflicts to disclose.

This article contains no studies with human or animal subjects performed by the authors.

References

Boquet, G., Boquet-Pujadas, A., Pisa, I., Dabak, A., Vilajosana, X., & Martinez, B. (2024). Indoor Position Estimation Using Angle of Arrival Measurements: An Efficient Multi-Anchor Approach with Outlier Rejection. *Internet of Things, 26*, 101236. https://doi.org/10.1016/j.iot.2024.101236

Chen, H., Yang, B., Li, L., Liu, T., Zhang, J., & Zhang, Y. (2025). Optimization-Based UWB Positioning with Multiple Tags for Estimating Position and Rotation Simultaneously. *Biomimetic Intelligence and Robotics, 5*(2), 100210. https://doi.org/10.1016/j.birob.2025.100210

Chen, Y., Li, D., Li, Y., Ma, X., & Wei, J. (2017). Use Moving Average Filter to Reduce Noises in Wearable PPG During Continuous Monitoring. Paper presented at the eHealth 360°, *Lecture Notes of the Institute for Computer Sciences, Social Informatics and Telecommunications Engineering, 181*, 193–203, Springer, Cham. https://doi.org/10.1007/978-3-319-49655-9_26

Cho, J., Jeong, S., Kim, J.-Y., Kim, G.-H., Lee, J., & Lee, B. (2025). Real-Time Indoor Localization and Safety Applications Using UWB in Construction. *KSCE Journal of Civil Engineering, 29*(8), 100164. https://doi.org/10.1016/j.kscej.2025.100164

Decawave (2021). DW1000 user manual, how to use, configure and program the DW1000 UWB transceiver. Decawave Limited Company (Ed.), (2.18 ed.). China.

Esmaeili-Yadaki, M., & Khani, H. (2024). X-Law Operation for Energy-Efficient Time-of-Arrival Positioning to Achieve Higher Accuracy with Lower Bandwidth: A Game-Changer for UWB Localization Devices. *ICT Express, 10*(6), 1179–1185. https://doi.org/10.1016/j.icte.2024.10.001

Han, Y., Zhang, X., Lai, Z., & Geng, Y. (2021). TOF-Based Fast Self-Positioning Algorithm for UWB Mobile Base Stations. *Sensors, 21*(19). https://doi.org/10.3390/s21196359

Hassan, S. K., H. Sallomi, A. H., & Wali, M. H. (2022). Design of a Dual-Band Rejection Planar Ultra-Wideband (UWB) Antenna. *Journal of Engineering and Sustainable Development, 26*(4), 30–35. https://doi.org/10.31272/jeasd.26.4.3

Huang, S., Guo, Y., Zha, S., Wang, F., & Fang, W. (2017). A Real-Time Location System Based on RFID and UWB for Digital Manufacturing Workshop. *Procedia CIRP, 63*, 132–137. https://doi.org/10.1016/j.procir.2017.03.085

Janousek, P., Slanina, Z., & Walendziuk, W. (2024). Target-Following Robotic Platform Based on UWB Localization and Depth Camera. IFAC-PapersOnLine, 58(9), 247–252. https://doi.org/10.1016/j.ifacol.2024.07.404

Koreis, J., Loske, D., Klumpp, M., & Glock, C. H. (2025). We Belong Together - A System-Level Investigation Regarding AGV-Assisted Order Picking Performance. *International Journal of Production Economics, 282*, 109527. https://doi.org/10.1016/j.ijpe.2025.109527

Kubasakova, I., Kubanova, J., Benco, D., & Kadlecová, D. (2024). Implementation of Automated Guided Vehicles for the Automation of Selected Processes and Elimination of Collisions between Handling Equipment and Humans in the Warehouse. *Sensors, 24*(3), 1029. https://doi.org/10.3390/s24031029

Li, P., Wu, W., Zhao, Z., & Huang, G. Q. (2024). Indoor Positioning Systems in Industry 4.0 Applications: Current Status, Opportunities, and Future Trends. Digital Engineering, 3, 100020. https://doi.org/10.1016/j.dte.2024.100020

Lyu, Y., Wei, M., Li, S., & Wang, D. (2025). A Fusion Positioning System with Environmental-Adaptive Algorithm: IPSO–IAUKF Fusion of UWB and IMU for NLOS Noise Mitigation. Measurement: *Sensors, 38*, 101864. https://doi.org/10.1016/j.measen.2025.101864

Ma, W., Fang, X., Liang, L., & Du, J. (2024). Research On Indoor Positioning System Algorithm Based On UWB Technology. *Measurement: Sensors, 33*, 101121. https://doi.org/10.1016/j.measen.2024.101121

Mo, J., & Lee, J. (2011). RFID-Based Indoor Positioning System. *International Journal of Radio Frequency Identification Technology and Applications, 3,* 141–154. https://doi.org/10.1504/IJRFITA.2011.039788

Qorvo (2025). DW1000 Ultra-Wideband (UWB) Transceiver IC with One Antenna Port. Retrieved from https://www.qorvo.com/products/p/DW1000#documents

Rajab, A. M., & Wang, B. (2024). Autonomous and Reliable Fingerprint Map Maintenance for Indoor Positioning System. *Computer Networks, 251*, 110626. https://doi.org/10.1016/j.comnet.2024.110626

Ranjan, R., Shin, D., Jung, Y., Kim, S., Yun, J., Kim, C., …, Kye, J. (2024). Comparative Analysis of Integrated Filtering Methods Using UWB Localization in Indoor Environment. *Sensors, 24*(4), 1052. https://doi.org/10.3390/s24041052

Ruiz, A., Garrido, J., Vázquez, F., & Ruz, M. L. (2024). UCO DWM1001: A tool for managing and processing the UWB DWM1001-DEV development board. *SoftwareX, 27*, 101848. https://doi.org/10.1016/j.softx.2024.101848

Saeidi, T., Mahmood, S. N., Saleh, S., Timmons, N., Al-Gburi, A. J. A., & Razzaz, F. (2025). Ultra-Wideband (UWB) Antennas for Breast Cancer Detection with Microwave Imaging: A Review. *Results in Engineering, 25*, 104167. https://doi.org/10.1016/j.rineng.2025.104167

Saengudomlert, P., Ubolkosold, P., & Sterckx, K. L. (2025). Development of a Position and Orientation Estimation System Using Extended Kalman Filtering for Indoor Visible Light Positioning. *AEU - International Journal of Electronics and Communications, 192*, 155684. https://doi.org/10.1016/j.aeue.2025.155684

Sakpere, W., Adeyeye Oshin, M., & Mlitwa, N. (2017). A State-of-the-Art Survey of Indoor Positioning and Navigation Systems and Technologies. South African Computer Journal, 29, 145. https://doi.org/10.18489/sacj.v29i3.452

Sanchez, A., de Castro, A., Elvira, S., Glez-de-Rivera, G., & Garrido, J. (2012). Autonomous Indoor Ultrasonic Positioning System Based on a Low-Cost Conditioning Circuit. *Measurement, 45*(3), 276–283. https://doi.org/10.1016/j.measurement.2011.12.002

Smith, S. W. (1999). The Scientist and Engineer's Guide to Digital Signal Processing (2nd ed.). San Diego, California: California Technical Publishing.

Sullivan, B. P., Yazdi, P. G., Suresh, A., & Thiede, S. (2022). Digital Value Stream Mapping: Application of UWB Real Time Location Systems. *Procedia CIRP, 107*, 1186–1191. https://doi.org/10.1016/j.procir.2022.05.129

DOI: 10.5614/j.eng.technol.sci.2026.58.4.4

Tran, V.-K., Thai, B.-T., Pham, H., Nguyen, V.-K., & Nguyen, V.-K. (2024). A Proposed Approach to Utilizing ESP32 Microcontroller for Data Acquisition. *Journal of Engineering and Technological Sciences, 56*(4), 474–488. https://doi.org/10.5614/j.eng.technol.sci.2024.56.4.4

Wang, H., Liang, C., Wang, G., & Li, X. (2024). Energy-Saving Potential of Fresh Air Management Using Camera-Based Indoor Occupancy Positioning System in Public Open Space. *Applied Energy, 356*, 122358. https://doi.org/10.1016/j.apenergy.2023.122358

Wang, Z., Li, S., Zhang, Z., Lv, F., & Hou, Y. (2018). Research on UWB Positioning Accuracy in Warehouse Environment. *Procedia Computer Science, 131*, 946–951. https://doi.org/10.1016/j.procs.2018.04.231

Xu, N., Guan, M., & Wen, C. (2025). A Survey on Ultra Wide Band Based Localization for Mobile Autonomous Machines. *Journal of Automation and Intelligence, 4*(2), 82–97. https://doi.org/10.1016/j.jai.2025.02.001

Zhang, Y., Chu, Y., Fu, Y., Li, Z., & Song, Y. (2022). UWB Positioning Analysis and Algorithm Research. *Procedia Computer Science, 198*, 466–471. https://doi.org/10.1016/j.procs.2021.12.271

Manuscript Received: 20 May 2025
Revised Manuscript Revision Received: 11 August 2025
Accepted Manuscript: 21 April 2026